

# Scaled hollow-cylinder tests for studying size effect in fracture processes of concrete

A.S. Elkadi

*Microlab, Faculty of Civil Engineering, Delft University of Technology, Delft, Netherlands*

J.G.M. van Mier

*Institute for Building Materials (IBWK), ETH Hönggerberg, Zürich, Switzerland*

**ABSTRACT:** We performed test series on scaled thick-walled cylinders in a size range 1:8 as part of an ongoing investigation concerned with size effect and fracture processes in weak quasi-brittle materials subject to multiaxial compressive stress. Two material mixtures, viz. 2 mm mortar and 4 mm concrete, have been tailored as model materials in these tests. In this paper, test results for size effect experiments are presented and discussed. Fracture processes revealed from impregnated specimens are explored and discussed as well. Concrete specimens have showed a size effect with respect to the external hydrostatic stress needed to initiate failure, whereas for mortar specimens, only small size specimens showed a size effect that vanished for larger sizes. Fracture observations suggest a splitting type of failure as the initial failure mechanism around the inner-hole for both concrete and mortar. Furthermore, in the mortar a bifurcation of failure and localization into shear-like fractures has been observed as well.

**Keywords:** size effect, multiaxial compression, hollow-cylinder test, fracture mechanism.

## 1 INTRODUCTION

A salient property of fracture of quasi-brittle heterogeneous materials, such as concrete and rock, is the size effect. An appreciable amount of experimental data on size effect can be found in literature, which mainly focus on direct tension, bending, and uniaxial compression (see e.g. Bazant & Chen 1997 for reference list). These data are routinely used for developing and validating numerical material models of fracture and size effect. Establishing realistic macroscale fracture or size effect models, however, requires an insight into the mesoscale crack mechanisms. According to Van Mier (1997), size effect in fracture of heterogeneous materials is an automatic outcome from mesoscale analyses where both structural effects (i.e. stress/strain gradients, boundary conditions, etc.) and material effects blend in a natural way. At this scale, heterogeneity results in stress and strain gradients that interact with the structural stress and strain gradients. In addition, it is considered better to use fracture geometry other than that used in model development for its tuning and validation. In this respect, three dimensionally

scaled experiments, performed under multiaxial compressive loading are yet a challenging option.

To date, only few and limited experimental data exists for size effect in multiaxial compressive fracture of concrete and rock. The effect of confining pressure on the size-strength relations and fracture propagation is missing substantial experimental background. Laboratory experiments using model openings such as scaled hollow cylinders are suited for such an investigating. The hollow cylinder geometry lends it self for providing permutations of various multiaxial states of stress around its inner-hole depending on the stress path applied to its external boundaries. Such test geometry is almost routinely used as a model test in studying stability of underground tunnels and deep oil boreholes. The size dependency of hollow cylinder strength, however, has received less consideration. Results are available for weak (Kooijman 1991, van den Hoek et al. 1992, Ringstad et al. 1993, Tronvoll & Fjaer 1994) and tight sandstones (van den Hoek et al. 1994). From these experiments, a trend of decreasing hollow cylinder strength with increasing inner-hole size was reported. The results also suggest that hollow

cylinder size effect is material-dependent and might be linked to associated fracture mechanisms.

The aim of our ongoing research is to carefully simulate and observe fracture processes and size dependency in hollow cylinder tests on concrete and mortar. This is achieved through performing experiments on scaled thick-walled cylinders of tailored concrete and mortar mixtures. In this paper, preliminary experimental results are presented and discussed for two test series of different heterogeneity level, viz. 2 and 4 mm maximum aggregate size. Attention is given to the fracture mechanisms that are observed during the impregnation experiments on fractured specimens. After describing the experimental facilities, material development and characteristics, the results are presented accompanied by a discussion, which focuses on the hollow-cylinder size dependence and observed fracture behaviour.

## 2 EXPERIMENTAL CONFIGURATION

### 2.1 Specimens

Test series have been performed on concrete hollow-cylinders with an inner diameter of 12.5, 25, 50, and 100 mm, i.e. a size range 1:8. All of the specimens have an inner-diameter / outer-diameter / length ratio of 1:4:6. In the remaining of this paper, specimens with inner-diameter of 12.5, 25, 50, and 100 mm are referred to as A, B, C, and D respectively. This would correspond to a wall thickness ( $W$ ) for each size equal to 18.75, 37.5, 75, and 150 mm respectively. The wall thickness in a hollow-cylinder specimen represents the smallest structural size.

### 2.2 High-pressure hollow-cylinder test setup(s)

Two hollow-cylinder test cells located at the petroleum laboratory (Dietzlab) of the Delft University of Technology were utilized for performing the experiments. One is a large hollow-cylinder cell, the borehole simulator, which was designed for simulating oil reservoir conditions down to nearly 3300 m depths. The cell accommodates solid samples with a diameter of 400 mm and a length of 600 mm with inner-hole diameter ranging from 60-100 mm. Both axial and radial pressures could be applied independently up to 40 MPa. As it is vital in any experimental investigation of size effect that all specimens be geometrically similar, and with similar boundary conditions, a second hollow-cylinder cell has been developed in close similarity with the existing one. The main difference is that the new cell capable of

accommodating hollow-cylinder specimens of 50, 100, and 200 mm outer-diameter.

In both cells, pumping oil into the cell via the upper connection in the top safety plate exerts the axial pressure. The resulting pressure is then transmitted via the plunger on to the sample. The radial pressure is applied by pumping oil via one of the oil inlets in the housing wall of the cell (Fig. 1). The oil pressure is transmitted as radial stress via a 2 mm thick NBR-rubber sleeve on to the specimen.

In order to monitor the deformation and failure propagation around the inner-hole, a special measuring device is developed. The device consists of two identical measuring arms with a measuring point at one end and the other end connected to a  $\pm 1$  mm stroke LVDT (Linear Variable Differential Transducer). The arms are connected to each other through a pivot that divides the distance between the measuring point and the LVDT to a known ratio. After preparing the specimen and cell for testing, the measuring device is positioned inside the inner-hole so that the measuring points are in contact with the specimen's walls at nearly mid height. As pressure is applied, the deformation occurring at the inner-hole is transmitted through the pivot to the LVDT that is connected to a PC.

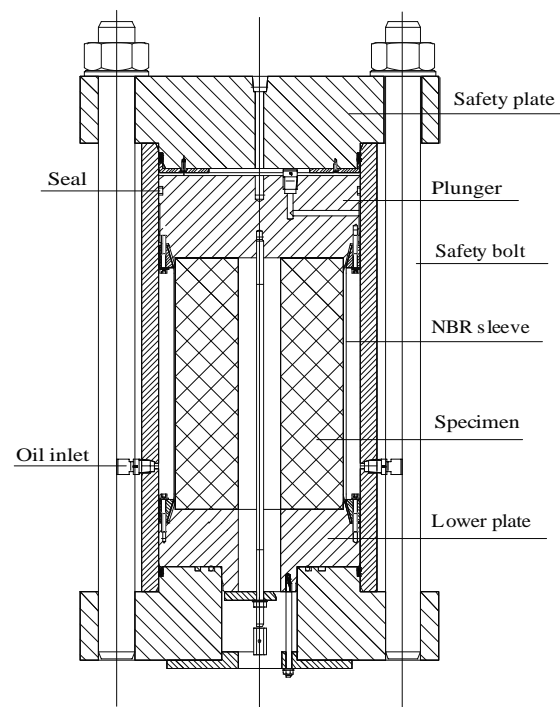


Figure 1. Schematic drawing of the triaxial test cell accommodating a hollow cylinder of size C.

For specimens of size C and D, in addition to measuring the radial deformation, the axial displacement of the top plunger is recorded as well. The limitation in measuring the axial displacement for only two sizes arises from the difficulty in accommodating the probe used for axial measurement beside the arms used for radial measurement in the relatively small holes for A and B specimens. During testing, the data collected from the calibrated pressure cells and measuring devices are scanned and recorded on a PC.

Fracture patterns, remaining after testing and after spalling that takes place, are preserved for post-mortem inspections. First, samples are inspected visually and pictures are taken through the open hole whenever possible. Then a fluorescent epoxy resin is impregnated in to the vicinity of the inner-hole under vacuum, which allows after hardening of the epoxy a careful study of the fracture patterns under UV (Ultra-Violet) light using optical microscopy. Typically, the specimen is sliced perpendicular to its axial axes in three equal parts. The central part is afterward cut diametrically and one of the two resulting pieces is once more cut diametrically in to two equal parts.

### 2.3 Experimental technique

The specimens are prepared by casting the concrete into cylindrical steel moulds, which are equipped with a centered steel core for providing the inner-hole configuration. A test series comprising all sizes plus twelve control cubes are cast from one batch. Six cubes are tested as reference cubes after 28 days for uniaxial compression and splitting tensile strengths. The other six cubes are tested within  $\pm 1$  day from the actual hollow-cylinder test date for control purposes. One day after casting, the inner-core is extracted, and later on the same day the complete samples are de-moulded and directly placed in a fog room at 95-99% relative humidity and 20° C temperature.

Depending on the planned time schedule for testing, cylinders are brought out of the curing room for preparation. First, the ends are ground flat and parallel to an accuracy of  $\pm 100$  micron to minimize end effects and to ensure good contact between loading platens and specimen. Due to the high w/c ratio used in mixtures plus casting in steel moulds, small to medium sized air voids are found on the outer surface of the specimens. These superficial voids present a considerable experimental complication as under high pressures, the rubber sleeve is pushed into these holes leading to its puncturing. This allows oil to travel through the specimen, which brings the test for immediate

termination due to pressure loss and specimen contamination with oil. Therefore, after manually brushing the specimen's outer surface with a steel brush, the surface is always treated with a low stiffness epoxy for filling the air voids.

The sample assembly is then placed between the top and bottom plates. The sleeve is stretched along the outer surface and fixed through two fixing rings to the top and bottom plates. For minimizing any possible frictional stresses, principally at low confining pressures, between specimen and platens, a friction reducing material is used. A sandwich layer comprising two Teflon sheets of 0.1 mm thickness each and a grease layer of 0.05 mm thickness in between is used (van Vliet & van Mier 1995). The assembly is placed inside the triaxial cell, which is filled with hydraulic oil and sealed for testing.

### 2.4 Loading and stress path

A variety of load paths can be applied in a hollow-cylinder test by changing the external pressures and/or the internal pressure. In order to simulate failure of deep boreholes, where instabilities are usually being induced by excessive hoop stress on the borehole wall, an external hydrostatic stress path is used in our testing. In all tests, the inner-hole pressure is kept equal to atmospheric. Specimens are loaded either to failure or up to the maximum capability of the testing cell corresponding to 40 MPa. At this stage, however, quite some local damage has occurred around the inner-wall of the cylinder.

In Figure 2, the hollow-cylinder geometry is schematized together with the load configuration used in our testing. Under a hydrostatic stress path, the  $P_{axial}$  and  $P_o$  are equally applied to the specimen. This external hydrostatic pressure would translate into triaxial stress gradients over the thickness of the wall with  $\sigma_\theta$  = tangential stress,  $\sigma_r$  = radial stress, and  $\sigma_z$  = axial stress. A linear-elastic solution for stresses and deformations for a hollow-cylinder geometry subjected to external boundary pressures can be found in any textbook on rock mechanics or solid mechanics (e.g. Jaeger & Cook 1979). This solution suggests that under plain strain conditions and hydrostatic external pressure with zero inner-hole pressure, maximum stress gradients would develop around the wall of the inner-hole with  $\sigma_\theta > \sigma_z > \sigma_r$ . Therefore, failure is expected to initiate around the inner-hole and propagate outwards. The linear elastic solution, however, does not account for size effect and is generally observed to underestimate the strength capacity of hollow cylinders (Santarelli 1987).

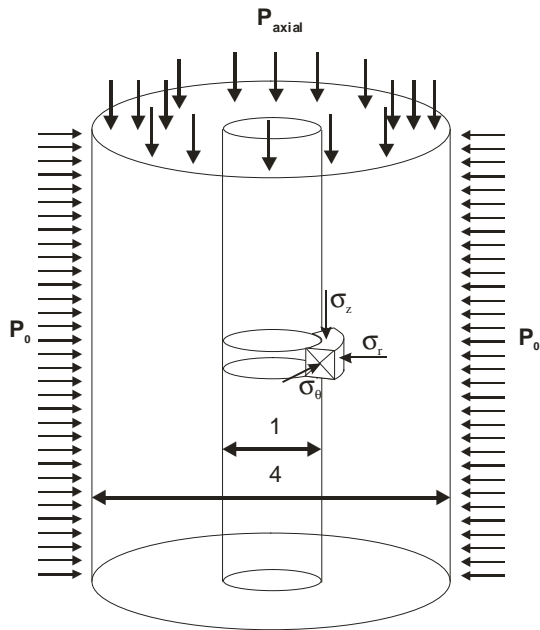


Figure 2. The hollow-cylinder geometry and loading configuration used in testing.

### 3 MATERIAL DESCRIPTION

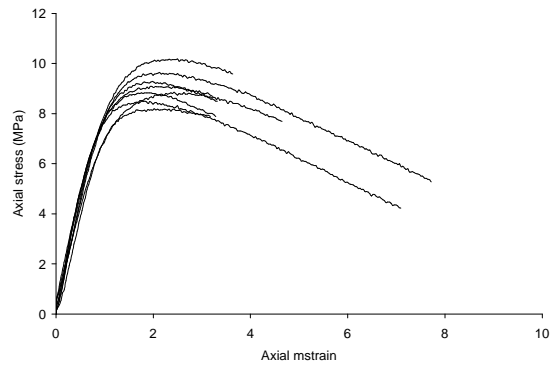
#### 3.1 Material design

A model material is developed to facilitate investigating the effect of aggregate size on size effect and failure mechanisms for weak quasi-brittle materials subject to multiaxial compressive stress. The material is designed to model weak rocks, mostly weak sandstones, where borehole instabilities often occur. A trial and error procedure was utilized for the design and preparation of the mortar with a target compressive strength of about 10 MPa. This target strength was set to simulate weak sandstones, such as Castlegate sandstone. A gap-graded concrete mixture is used comprising two-aggregate grain sizes at a grain diameter ratio 6:1 and a ratio, by weight, of the large to small grains of approximately 3:1. Ordinary Portland cement of type CEM I 32.5R was used at a ratio of 10-11% by weight and a water/cement (w/c) ratio of 0.8. Several mixtures were investigated of various maximum aggregate sizes (Elkadi et al. 2002). For minimizing wall effects and maintaining a ratio ~5 between the maximum aggregate size and the smallest structural size of specimen A (18.75 mm), the 2 and 4 mm mixtures have only been considered for testing.

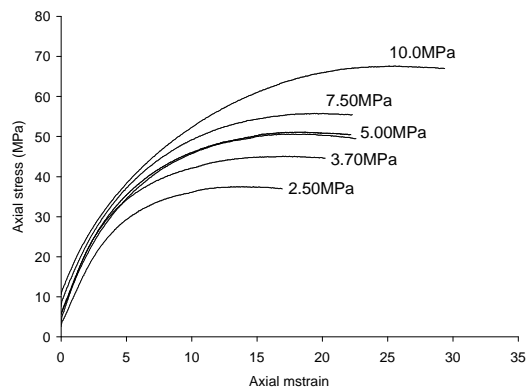
#### 3.2 Material properties

The density and effective porosity were determined using Helium pycnometry resulting in dry densities in the range of 2400-2600 kg/m<sup>3</sup> with 16-17% effective porosity.

The constitutive behaviour of the material, both the 2 and 4 mm mixtures, could be described as quasibrittle under uniaxial compression to plastic-strain-hardening when subject to moderate to high confining stresses. Under uniaxial compression, the material exhibits a typical quasi-brittle behaviour with a nearly linear ascending branch up to ~80% of the peak stress (Fig. 3a). Afterwards, dilatancy takes place with an increase in lateral displacement until failure. Post peak, a slowly descending branch is observed. In triaxial testing, large plastic strains could be supported without significant macroscopic failure (Fig. 3b).



(a)



(b)

Figure 3. Results of 8 uniaxial compression tests for the 4 mm mixture (a) and results of 6 triaxial compression tests for the same mixture at various confining pressures indicated beside the stress-strain curves (b).

With application of a small confining stress, during triaxial testing, strengthening was observed and the material behaved in a plastic-strain-hardening manner. The high water/cement ratio used in the mixtures resulting in a porous material structure with sizeable air voids is thought to be of an important influence on the observed constitutive behavior of the material.

In Table 1, major mechanical properties for the 4 mm mixture are given. These are the uniaxial compressive strength, Poisson's ratio, and the Young's modulus as revealed from the fully instrumented uniaxial compressive tests on solid cylindrical samples (Fig. 3a). In addition, the splitting tensile strength is given, which is calculated from Brazilian test results performed on disk shaped specimens.

Table 1. Mechanical properties of the concrete

Property	Value
	MPa
Uniaxial compressive strength	$9.10 \pm 0.60^*$
Splitting tensile strength	$1.10 \pm 0.20^*$
Poisson's ratio**	$0.15 \pm 0.01^*$
Young's modulus ( $\times 10^{-3}$ )	$7.70 \pm 0.60^*$

\* Standard deviation value

\*\* Dimensionless quantity

## 4 RESULTS AND DISCUSSION

### 4.1 Stresses and strains

Two completed series of experiments are considered next. One comprising the four sizes from the 4 mm concrete and second including A, B, and C sizes only from the 2 mm mortar. In Figure 4, a typical external stress vs. tangential inner-hole strain curve is shown. From the principles of linear elasticity, the tangential strain at the inner-wall is directly derived from the radial deformation measurements through dividing their value by the inner radius. This tangential strain is considered the maximum principal strain as it corresponds to the maximum principal stress ( $\sigma_\theta$ ). Measured external pressures are converted to stresses using linear elasticity and used for analysis and interpretation as commonly done in hollow-cylinder tests.

From Figures 3-4, the material is shown to behave in a plastic-strain-hardening manner. The uniaxial compressive strength for the specimen shown in Figure 4, from accompanying control cubes, is 10.7 MPa. This specimen sustained external pressures up to 32.5 MPa without complete collapse. Nevertheless, the measured tangential strains are noticeably high, in the order of few percents. A feature of all stress-strain curves

obtained from all sizes tested so far is the soft transition from an initial slightly curved to the subsequent much softer response. This soft transition makes it very difficult, practically impossible, to define a stress point that could be regarded as onset of microcracking or failure. In a more brittle-like material tested under confining stress less than the brittle-ductile transition, onset of cracking is commonly considered the point where the stress-strain curve deviates from its initial linear branch. In Figure 4, the axial strain calculated from the measured axial deformation for the same test is given as well. The value of axial strain is much less as compared to the tangential one and the response is noticeably stiffer.

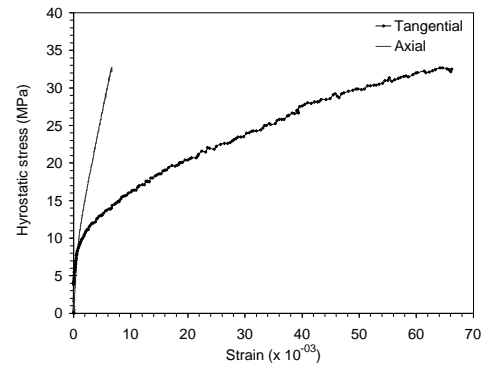


Figure 4. A representative stress-strain plot for specimen C of the 2 mm mortar. The applied external stress (MPa) versus both the axial and tangential strains (mstrain) are shown.

### 4.2 Fracture observations

Over the past two decades, hollow cylinder test results on rock, and concrete have established that failure around the inner-wall is governed by either tensile (splitting) or shear type failure mechanisms. In this respect, shear failure is described macroscopically by spiralling shear bands that originates at the inner-wall. At the microscale, unresolved debates exist over the shear fracture initiation. Tendency of a certain material to follow one of these mechanisms in hollow cylinders is yet poorly understood and contradictory observations have been reported (van den Hoek et al. 1994).

Results from our impregnation experiments suggest that the initial failure mechanism in 4 mm concrete is the so-called splitting failure mode. In this case, fracturing is characterized by small splitting cracks distributed all round the inner-wall in a concentric pattern. The cracks are generally located parallel to the inner-wall, which coincides with the direction of maximum principal stress  $\sigma_\theta$ .

The depth of this damage zone ranged from 5 to 18 mm for the A and D sizes respectively. Depending on the grain mineralogy and/or grain orientation relative to the direction of principal (tangential) stress, both inter- and intra-granular cracks are formed (Figs. 5-6). As regards the 2 mm mortar, the above observations generally pertain with an addition that observed damage is more extensive. Fractures observed in sections perpendicular to the vertical axes reveal a concentric damage pattern (Fig. 5) with short microcracks located generally parallel to the inner-wall. No breakout formation is observed as often seen in testing of rock materials. This may indicate that anisotropy in strength of material and/or stress anisotropy could be the source of localized breakout formation. Therefore, the use of breakout data from deep boreholes for identifying stress directions and magnitudes should be approached with caution.

A preliminary analysis of the fracture process from our observations for both materials is that firstly, small splitting cracks initiate very close to the inner-wall in a concentric pattern. Then, with stress increase, more cracks form deeper in from the wall. Depending on the grain size, grain stiffness with respect to orientation of crack propagation, and grain/matrix strength ratio, cracks would propagate either inter- or intra-granularly parallel to the principal stress direction (Fig. 6). For the 2 mm mortar, inter-granular crack propagation seems preferable as cracks could meander around grain boundaries with much less energy when compared to the 4 mm concrete. In the later case, if grain strength is close to or less than matrix strength cracks could propagate intra-granularly under increasing stress levels. In both materials, however, the matrix strength is relatively low as compared to normal strength concretes due to its high porosity resulting from high w/c ratio used. This low matrix strength results in grain boundaries as being a favorable crack nucleation and propagations sites. The damage zone does not extend very deep in the wall and much higher pressures are probably needed to bring the specimens to a collapse. A collapse would be expected to correspond to a damage zone extending out to the external boundaries of the specimens. The observed limited expansion of damage is believed to be due to the strengthening effect of the radial stress away from the inner-wall. In other words, stress gradients over the wall could be crucial in determining the extent of damage. The foregoing postulated fracture process is very much in line with observations by Ewy & Cook (1990).

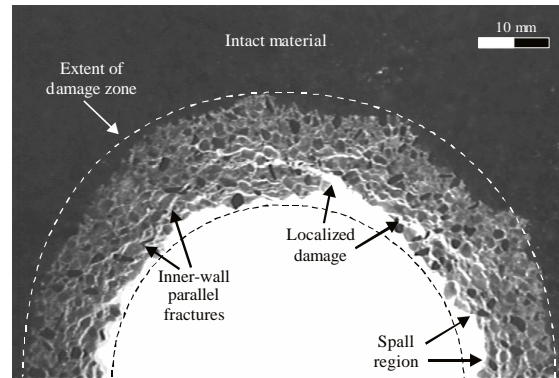


Figure 5. Partial section of a C specimen from the 2 mm mortar at nearly 1/3 length from bottom, showing fracture pattern at 32.5 MPa external pressure.

A noteworthy observation for specimen C of the 2 mm mortar is the activation of a shear-like mechanism with formation of spiral fractures that intersect the surface of the inner-wall as localized damage (Fig. 5). It seems that when circumstances allow, in terms of stress, material structure, and size, bifurcation of the deformation process could be a characteristic effect. For the 4 mm concrete and specimens A and B from the 2 mm mortar, however, localization of damage has not been witnessed. Nevertheless, it should not be excluded for more observations are still necessary.

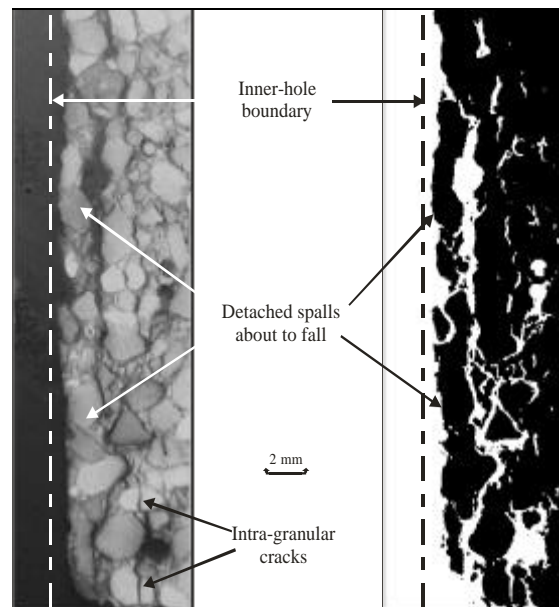


Figure 6. Partial longitudinal section for B specimen from the 2 mm mortar, showing spalling and cracking.

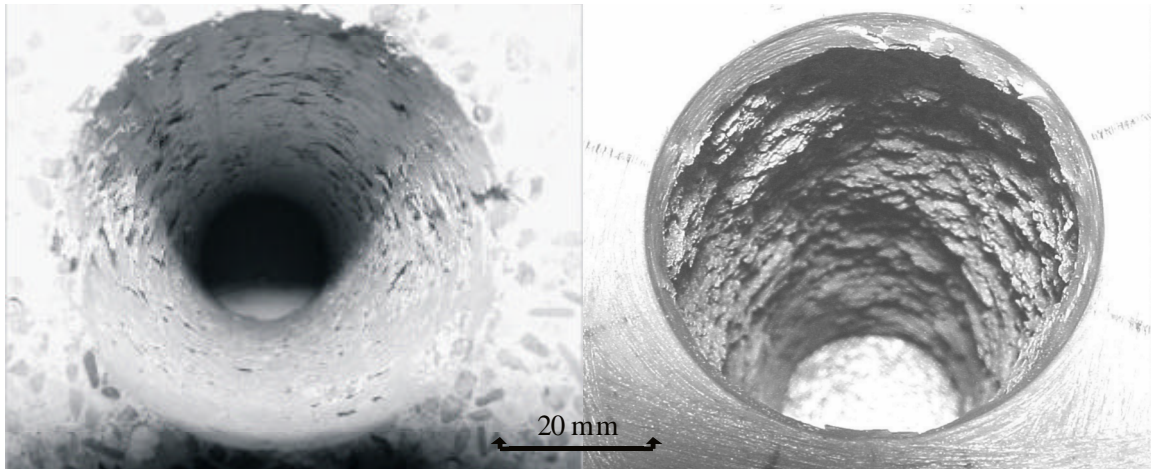


Figure 7. Appearance of specimens size C at completion of the tests (35-37 MPa) for 4 mm concrete (left), and 2 mm mortar (right).

Observations from sections sliced parallel to the axial axes are in accordance with the statements just before regarding the fracture process. Spalls that are detached and ready to fall are clearly visible (Fig. 6). Visible as well are the short microcracks parallel to the inner-wall, which run both inter- and intra-granularly. The observed spalls are generally thin slabs with a finite thickness in the order of 1-2 grain size and finite length in the order of 5-10 times grain size. During testing, more spall activities were observed for the 2 mm mortar as compared to the 4 mm concrete.

Pictures taken inside open inner-holes just after testing (Fig. 7) show the difference in spalling activities for specimen type C from the two mixtures. In the 4 mm concrete, small slivers are detached and intact material remain, whereas the 2 mm mortar shows much more spall regions with hardly any intact material left. Failure in mortar shows warping of the surface in an undulating way. Both materials, however, show damage over the whole sample length and all around the inner-hole.

#### 4.3 Size effect

Figure 8 gives the size-stress relation from performed two test series. A log-stress versus log wall-thickness ( $W$ ) is given wherein the stress value corresponds to a tangential strain value equal to five mstrain. This is a somewhat arbitrary strain value, which is used for comparison purposes. In the 4 mm series, alas, some problems occurred with the hydrostatic pressure application during testing of the C specimen. A specimen of the same size from another batch was used for test repetition and its test result is utilized for analysis in Figure 8.

A decrease in the hollow-cylinder strength with an increase in the cylinder size is observed for the 4 mm concrete. The trend for the 2 mm mortar is less obvious, although specimen A is apparently stronger than specimens B and C where the size effect vanishes. The UCS for the 4 mm at time of testing is 16 MPa, whereas for the 2 mm is 10 MPa. The difference in size-strength response for the two materials is not clear at this point if dependent on difference in UCS, heterogeneity level, failure mechanisms, a combination of these, or an experimental artifact. However, fracture mechanism and heterogeneity scale are apparently linked and the vanishing size effect in the 2 mm mortar for  $W$  sizes greater than 37.5 mm could possibly be attributed to these factors.

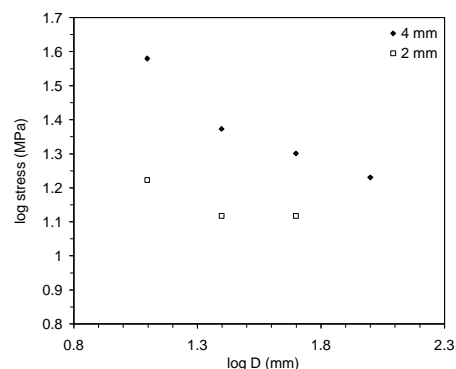


Figure 8. The Log-stress (MPa) versus log-wall thickness (mm) relation for the 4 and 2 mm mixtures. Stress values shown are the ones needed to bring a 5 mstrain tangential strain in the specimens at its inner-wall.

In terms of fracture mechanisms, similar observations have been reported by (van den Hoek et al. 1994) where the size effect for large tight Berea sandstone specimens ( $W > 30$  mm) was much less than for smaller holes. Van den Hoek et al. (1994) reported from their experiments on Berea sandstone hollow cylinders that failure of the large specimens is governed by shearing, whereas in the smaller specimens by preference for splitting. They argue that shear failure is generally less size dependent as compared to splitting failure and this could be the reason for the vanishing size effect in large specimens. If this applies to our material (with considerably larger grain size as compared to Berea sandstones) is subject to further experimental investigation. The experiments would include a variety of final stress states to establish carefully the fracture sequence.

## 5 CONCLUSIONS

Scaled thick-walled cylinder tests of two concrete mixtures, viz. 2 mm mortar and 4 mm concrete, indicates a size dependence for the hollow cylinder strength. The 2 mm mortar is found to be less size dependent when compared to the 4 mm concrete where the size effect vanished for large sizes.

Fracture observations suggest that a splitting mode is the initial failure mechanism for the tested materials. Bifurcation/localization in to shear-like fractures have been observed as well but only for large size specimen from the 2 mm mortar. The condition(s), which allow(s) for this localization to occur is subject to ongoing investigation.

Three dimensional size effect experiments under complex geometric and loading conditions as provided by the hollow cylinder test appears as a powerful tool for exploring and understanding fracture mechanisms in quasi-brittle materials. This could further assist in validating fracture models and identifying material parameters to describe material behaviour.

## 6 ACKNOWLEDGEMENTS

We are indebted to Ing. G. Timmers for his expert help in designing and performing the experiments. The financial support by the Dutch Technology Foundation (STW) is acknowledged.

## 7 REFERENCES

- Bazant, Z.P. Chen, E.P. 1997. Scaling of structural failure. *Applied mechanics reviews*, 50(10): 593-627.
- Elkadi, A.S., van Mier, J.G.M. & de Pater, C.J. 2002. Development and Behaviour of Low-Strength Concrete. 4<sup>th</sup> International Ph.D. symposium in Civil Engineering, Munich, Germany, 1: 135-142. Springer-VDI-Verlag GmbH.
- Ewy, R.T. & Cook, N.G.W. 1990. Deformation and fracture around cylindrical openings in rock-II. Initiation, growth and interaction of fractures. *Int. J. Rock Mech. Min. Sci. & Geomech. Abstr.*, 27(5): 409-427.
- Jaeger, J.C. & Cook, N.G.W. 1979. *Fundamentals of Rock Mechanics*. Science paperbacks 18. Chapman and Hall, London: 593.
- Kooijman, A.P., van den Elzen, M.G.A., & Veeken, C.A.M. 1991. Hollow-cylinder collapse: measurement of deformation and failure in an X-ray CT scanner, observation of size effect. *Rock Mechanics as a Multidisciplinary Science*, 657-666. Balkema, Rotterdam.
- Ringstad, C. et al. 1993. Scale effects in hollow cylinder tests. *2nd workshop on Scale effects in rock masses, Lisbon, Portugal, June, 1993*, 75-80. Balkema, Rotterdam.
- Santarelli, J.F. 1987. *Theoretical and experimental investigation of the stability of axisymmetric wellbore*. Ph.D. Thesis, Imperial College, London, 472 pp.
- Tronvoll, J. & Fjaer, E. 1994. Experimental study of sand production from perforation cavities. *International Journal of Rock Mechanics and Mining Science & Geomechanics Abstracts*, 31(5): 393-410.
- van den Hoek, P.J. et al. 1992. Size-dependency of hollow cylinder collapse strength. *SPE 67<sup>th</sup> annual technical conference and exhibition, Washington, DC*, 351-360.
- van den Hoek, P.J. et al. 1994. Size-dependency of hollow-cylinder stability. *EUROCK '94 - Rock Mechanics in Petroleum Engineering, Delft, The Netherlands, 29-31 August 1994*, 191-197.
- van Mier, J.G.M. 1997. *Fracture processes of concrete*. New directions in civil engineering. CRC Press, Boca Raton: 448.
- van Vliet, M.R.A. & van Mier, J.G.M. 1995. Softening behaviour of concrete under uniaxial compression. *Fracture Mechanics of Concrete Structures, FraMCoS-2, Freiburg, 383-396*. AEDIFICATIO Publishers.